Electronic Supplementary Information

In-plane molecular organization of hydrated single lipid bilayers: DPPC:cholesterol

Berta Gumí-Audenis,[a,b,c,d] Luca Costa,[e] Lorena Redondo-Morata,[f] Pierre-Emmanuel Milhiet,[e] Fausto Sanz,[b,a,d] Roberto Felici,[g] Marina I. Giannotti,[d,a,b,*] and Francesco Carlà[c,*]

[a]Institute for Bioengineering of Catalonia (IBEC), Barcelona, Spain. Email: migiannotti@ibecbarcelona.eu

[b]Materials Science and Physical Chemistry Department, Universitat de Barcelona, Barcelona, Spain

[c]ESRF, The European Synchrotron, Grenoble, France. Email: francesco.carla@esrf.fr

[d]Centro de Investigación Biomédica en Red (CIBER), Madrid, Spain

[e]Centre de Biochimie Structurale, CNRS UMR 5048 – INSERM UMR 1054, Montpellier, France.

[f]Unité 1006, INSERM, Aix-Marseille Université, FR-13009 Marseille, France

[g]Istituto SPIN-CNR, Roma, Italy.

ESI 1. Experimental

1.1. Materials

1,2-dipalmitoyl-*sn*-glycero-3-phosphocholine (DPPC) and cholesterol (chol), chloroform and methanol were purchased from Sigma-Aldrich (St. Louis, MO). 1,2-dipalmitoyl-*sn*-glycero-3-phosphoethanolamine-*N*-(lissamine rhodamine B sulfonyl) (DPPE-Rhodamine) was purchased from Avanti Polar Lipids Inc. All experiments were performed in buffer solution of 20 mM 4-(2-hydroxyethyl)-1-piperazineethanesulfonic acid (HEPES), 150 mM NaCl, 20 mM $MgCl_2$ (pH 7.4) prepared with ultrapure water (Milli-Q reverse osmosis system, 18.2 mΩ·cm resistivity) and filtered before use with an inorganic membrane filter (0.22 μm pore size Whatman International Ltd, England, UK).

1.2. Sample preparation

DPPC and chol were individually dissolved in chloroform:methanol (v:v 3:1) to give a final concentration of 3 mM. Aliquots of DPPC and chol solutions were mixed and poured into a falcon tube to obtain the different compositions (DPPC:chol 100:0, 90:10, 80:20, 60:40 and 50:50 molar ratio).[1] For the fluorescence measurements, the DPPC:chol solutions were subsequently mixed with DPPE-Rhodamine to obtain a final DPPE-Rhodamine molar fraction of 0.05 %. Next, the solvent was evaporated to dryness under nitrogen flow in order to achieve a thin film spread on the walls of the tube. The dried lipids films were then hydrated with buffer solution, previously heated above the transition temperature of the phospholipid, until a final total concentration of 0.5 mM. The falcon tubes were later subjected to cycles of vortex mixing and heating to *ca.* 60ºC. The vesicles suspensions were placed in an ultrasound bath for 30 min to finally obtain unilamellar vesicles.[2-4] For the fluorescence measurements, the vesicles were also extruded with a polycarbonate membrane filter (100 nm pore size, Whatman, purchased from Avanti Lipids).

Si wafers with orientation (100) ± 5º, polished (r.m.s. > 0.3 nm), 275 μm thickness with its native oxide and 50.8 mm diameter were purchased from CrysTec. Square substrates with approximate dimensions of 5 x 5 mm^2 were obtained from the wafers and cleaned with piranha solution (7:3 H_2SO_4:H_2O_2 (30%)). *Caution: Piranha solution should be handled with extreme caution*. Then, they were exposed to plasma (Expanded Plasma Cleaner PDC-002, Harrick Scientific Corporation) at high RF power level for 4 min to activate the hydrophilic bonding of the Si surfaces. The circular glass coverslips (3.5 cm diameter, 180 μm thick, purchased from WilcoWells) were cleaned with piranha solution and exposed at high RF for 15 min.

Supported lipid bilayers (SLBs) were obtained by vesicles fusion method.[1, 3, 5] The vesicles suspensions were deposited onto the corresponding substrate and incubated for 30 min at 70 ºC. Afterwards, the samples were rinsed several times with buffer solution to avoid unfused vesicles, always keeping the substrates hydrated.

1.3. Grazing incident X-rays diffraction (GIXD)

The GIXD experiments described here were conducted at the ID03 surface diffraction beamline of the ESRF, The European Synchrotron in Grenoble (France). The beam energy was 24 keV, corresponding to a wavelength of 0.516 Å, and the beam was focused at the sample position to a final size of 30 x 500 μm^2 (FWHM, vertical × horizontal). A MAXIPIX detector was installed on the diffractometer arm, 900 mm from the sample, with slits located 50 mm from the sample and with an opening of 4 mm x 2 mm (vertical x horizontal) to reduce the background level. The samples were directly mounted on the diffractometer stage. All the measurements were performed at room temperature in grazing incidence geometry with 0.05º incidence angle. To limit the exposure time and thus the possible beam damage during GIXD measurements, the scans were recorded by collecting a limited number of images in each scan. Typically, a scan from 2θ = 4 to 2θ = 8 was covered with 20 points. Raw data reduction was performed using the BINoculars code.[6] The data reported in Fig. 4 (main manuscript) were obtained by summing the intensities of each pixel along the direction parallel to $Q_{perpendicular}$ in an interval of $Q_{perpendicular}$ ranging from 0.02 to 0.15 $Å^{-1}$.

The access to high $Q_{perpendicular}$ values is limited by the geometry of the set-up and depends on the distance between the two silicon wafers and their surface size. In the present work we used two square silicon wafers with an area of 5x5 mm^2 laying at distance of 50 μm. Considering that the beam is hitting the system at the centre of the substrate, we can calculate that the maximum value of $Q_{perpendicular}$ accessible before the signal cut by the edge of the top Silicon wafer is ~ 0.19 $Å^{-1}$. This value could be probably augmented by increasing the distance between the wafers or reducing their size. The first option is not possible because it would lead to an increase of the thickness of the wetting layer and, thus, an increase in the background level. The reduction of the area of the wafers, for example by using rectangular samples with a shorter edge perpendicular to the direction of the beam, is a possibility that could be explored in the future. However, there might be some issues related to the evaporation of the solution near the edge of the sample and the homogeneity of the sample in the region close to the edge.

ESI 2. X-Rays (XR) measures: Sample alignment procedure

The Si-SLB sample was mounted on the diffractometer with its surface covered by a droplet of buffer solution. The surface tilt, as well as its vertical position, was then aligned parallel to the incident beam by rocking the sample tilt while monitoring the reflected intensity. Once XR beam and surface were aligned, the second Si substrate was positioned on top of the sample with its polished surface facing the sample. The liquid excess in the sample was spilled from the sides and carefully removed. The gap between the two Si wafers was estimated by measuring the transmitted intensity during a scan along the direction vertical to the sample surface. A typical scan used to estimate the gap size is reported in Fig. S1. It is worth noting that this method cannot be used for the exact determination of the gap size, because the value obtained in the transmission measure is a convolution of the gap width and beam size. The latter is too large to be used as a probe for an accurate estimation, however, the measure still provides reliable information about the maximum value of the gap size. The peak corresponding to the gap between the Si wafers reported in the Fig. S1 has a width at the base of 50 µm which is comparable with the width of the incidence beam (54 µm). Considering the convolution between the beam and gap size, we can conclude that in the vertical scan the sample is acting as a pinhole and the shape of the curve is in fact determined by the beam size, while the gap between the two Si wafers must have a size considerably smaller than 50 µm, probably about few microns or less.

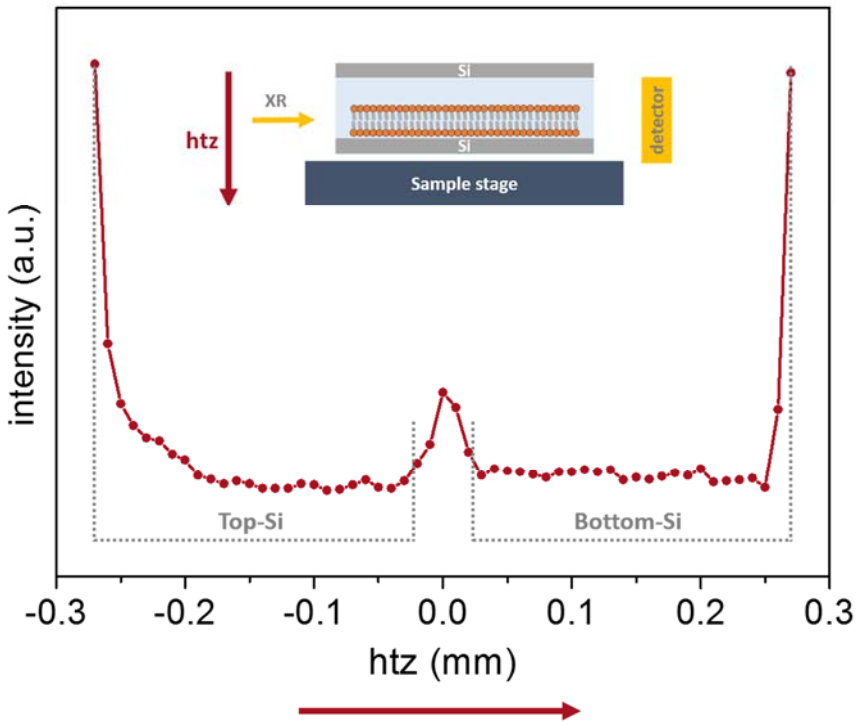

Fig. S1 XR transmission scan along the direction vertical to the Si-SLB-Si sample surface (htz). The transmission of the Si wafers is lower than that of the buffer and the gap between the two Si wafers can be identified as a peak at the center of the plot. At the outer edges of the Si wafer the transmission increases again, as observed for the top-Si/air interface and the bottom-Si/sample stage gap on the left and right edges of the plot, respectively. The increase of the intensity at the Si/stage interface is due to the presence of an XR transparent adhesive tape used to fix the sample. The nominal thickness of the wafers is 275 µm.

ESI 3. XR reflectivity (XRR)

An XRR curve for a pure DPPC bilayer onto a Si substrate (without the upper Si wafer), with a buffer droplet on top (as in Fig. 1(b)-I in the main text) is shown in Fig. S2, which validates the presence of a single gel-like state SLB, suggesting a membrane thickness of 5.9 nm, comparable to values already reported.[1, 2] For the acquisition of XRR scans, a set of attenuators was used to control the incident photon flux and limit the exposure of the sample to XR.

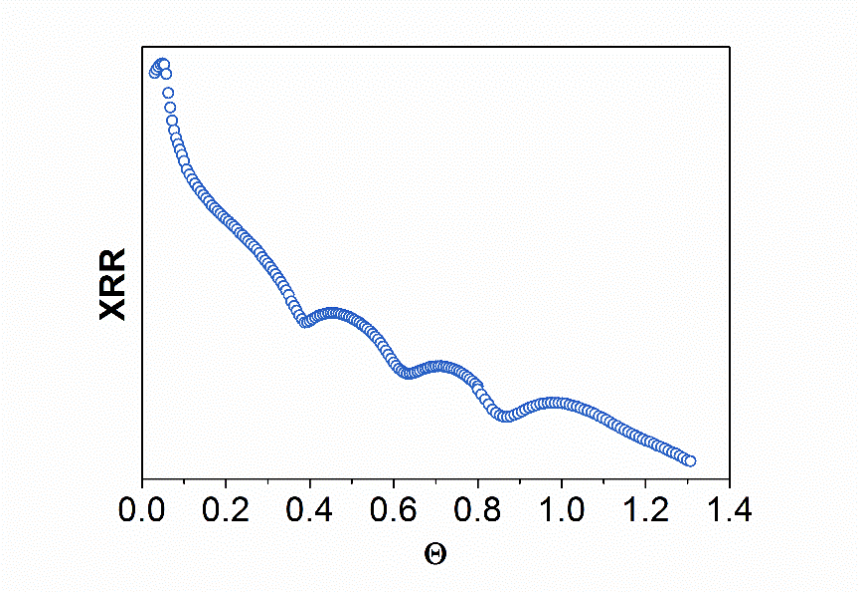

Fig. S2 XRR for DPPC SLB onto Si substrate, in 20 mM HEPES, 150 mM NaCl, 20 mM $MgCl_2$ buffer solution pH 7.4, at room temperature.

ESI 4. GIXD intensity

Due to a lack of homogeneity in the coverage of the SBLs, the diffraction intensity can vary depending on the azimuthal orientation and lateral positioning of the sample on the diffractometer stage. A series of GIXD measures collected on a DPPC SLB by rotating the sample over an angle of 150 degrees in steps of 30 degrees (Fig. S3) shows that while the peak positions in $Q_{parallel}$ remains constant, the intensity of the peak can vary significantly.

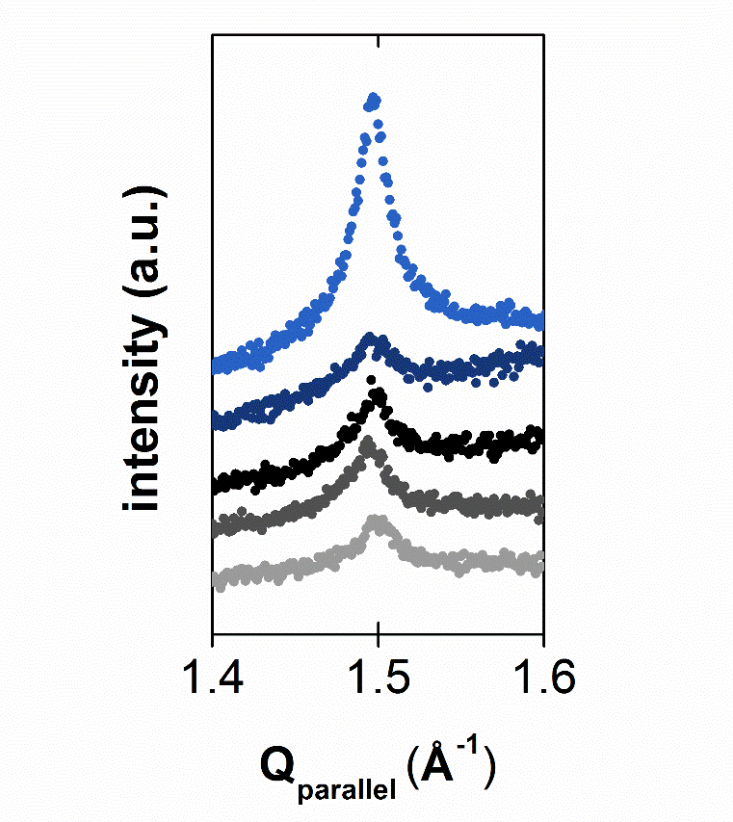

Fig. S3 GIXD $Q_{parallel}$ intensity (integrated over $Q_{perpendicular}$) patterns from a pure DPPC SLB in Si-SLB-Si configuration, acquired over a rotation of 150 degrees in steps of 30 degrees, in 20 mM HEPES, 150 mM NaCl, 20 mM $MgCl_2$ buffer solution pH 7.4, at room temperature.

ESI 5. Atomic Force Microscopy (AFM) and fluorescence microscopy measurements

We used AFM and Fluorescence microscopy to demonstrate that the phase behavior already observed for the DPPC:Chol system, either in liposomes, or in mica-SLBs, remains the same when the bilayer is deposited onto Si substrates.

ESI 5.1. AFM

AFM images were performed using an MFP-3D AFM (Asylum Research, Santa Barbara, CA). All AFM images were acquired in AC mode at room temperature under liquid conditions (buffer solution) using V-shaped Si_3N_4 cantilevers with sharp silicon tips and having a nominal spring constant of 0.35 $N \cdot m^{-1}$ (SNL, Bruker AFM Probes, Camarillo, CA).

AFM topographical images of the DPPC:chol SLBs at different concentrations (100:0, 90:10, 80:20, 60:40 and 50:50 molar ratio) are shown in Fig. S4. From the pure DPPC SLB topography (100:0 molar ratio), a bilayer thickness of about 5 nm can be determined from the section profile. This value is slightly lower than the one obtained by the XRR curve (5.9 nm) probably due to the membrane compression while scanning. As observed in Fig. S4, the bare Si substrate displays high roughness (r.m.s. > 0.3 nm). This makes difficult differentiating phase domains that are known to have a thickness difference of the same order ~ 0.2-0.3 nm^2 for DPPC:chol bilayers.

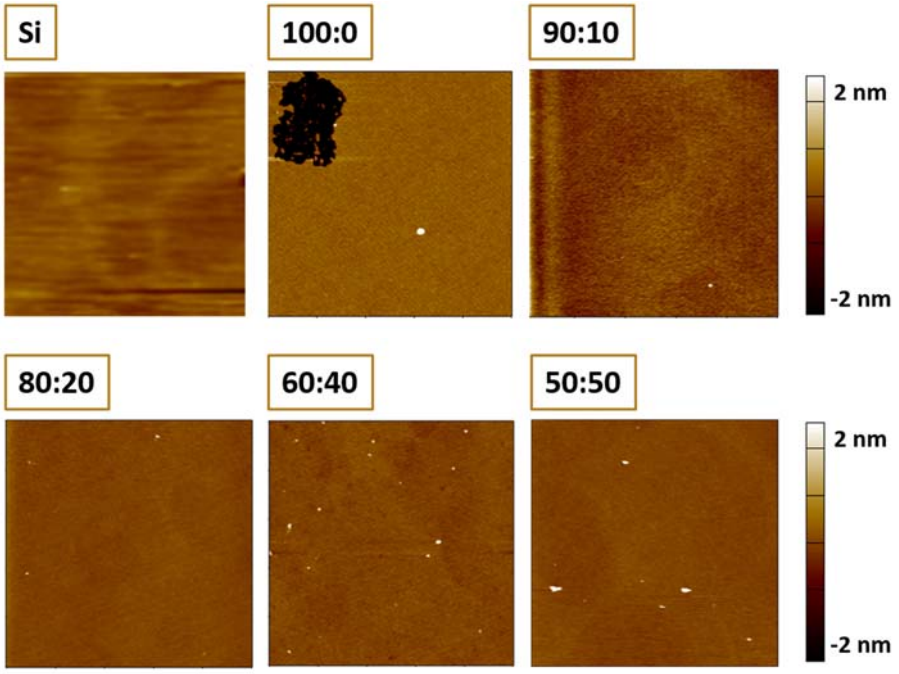

Fig. S4 5 x 5 μm^2 AFM images from Si and DPPC:chol SLBs (100:0, 90:10, 80:20, 60:40 and 50:50 molar ratios) on Si, in 20 mM HEPES, 150 mM NaCl, 20 mM $MgCl_2$ buffer solution pH 7.4, at room temperature.

ESI 5.2. Fluorescence microscopy

SLBs were imaged by fluorescence microscopy making use of a custom made inverted fluorescence microscope. We used an excitation wavelength of 525 nm and an emission filter centered at 605 nm (70 nm wide, CHROMA ET605/70). Fluorescence images were obtained with an externally-triggered iXon Ultra897 camera (Andor Technologies) with pulses of 100 ms period, resulting in an exposure time of 50 ms. Images were obtained by averaging over 20 single micrographs acquired in a row with ImageJ software. In order to reduce the background generated by the liquid environment, the Si substrate supporting the SLBs were turned upside down on top of a glass coverslip and imaged making use of an inverted objective.

Fluorescence images of DPPC:chol SLBs on Si, for 100:0, 90:10 and 60:40 molar ratio, are shown in Fig. S5, representing the different morphologies of the system. While an

expected homogeneous membrane was obtained for the pure DPPC bilayer, formation of chol-rich domains in the DPPC:chol 90:10 SLBs were clearly evidenced, in agreement with the phase segregation for low contents of chol. When increasing the chol content up to 40 mol %, domains are no longer observed, as expected for high chol contents.

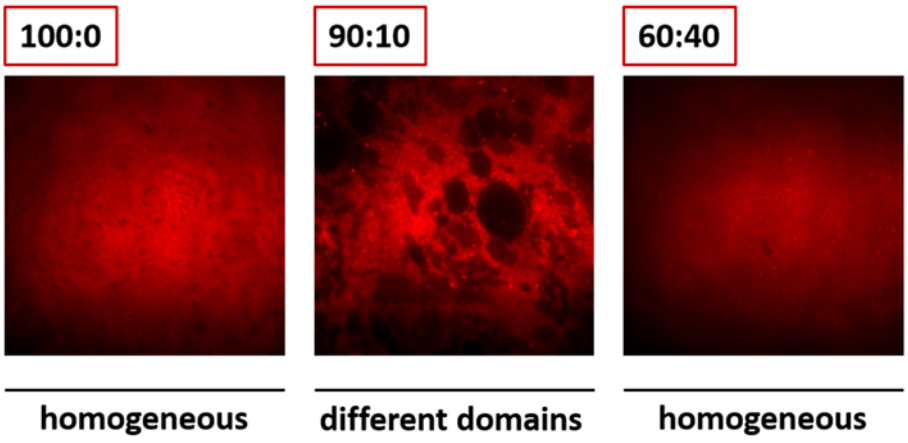

Fig. S5 55 x 55 μm^2 fluorescence images (512 x 512 pixels) from DPPC:chol mixed with 0.05 % DPPE-Rhodamine SLBs on Si, of 100:0, 90:10, and 60:40 molar ratios, in 20 mM HEPES, 150 mM NaCl, 20 mM $MgCl_2$ buffer solution pH 7.4, at room temperature.

ESI 5.3. Correlative AFM-Fluorescence microscopy

To identify the chol-rich and chol-poor regions in DPPC:chol SLBs with less than 30 mol % chol, we used a correlative AFM-fluorescence microscope (Nanowizard 4 combined with fluorescence microscopy, JPK, Germany) to associate the domains of a DPPC:chol (90:10 molar ratio) from the fluorescence image with the corresponding topographical information by AFM. All the measurements were performed at room temperature and under liquid conditions. The AFM images were acquired using V-shaped Si_3N_4 cantilevers with sharp silicon tips (MSNL, Bruker AFM Probes, Camarillo, CA) and by means of quantitative imaging (QI) mode. As Si substrates are not transparent to visible light, SLBs were formed by vesicle fusion onto glass.

Fig. S6 shows that membrane regions with higher thickness (AFM, left), previously identified as chol-rich domains,[1] correlate well with regions with lower fluorescence intensity (fluorescence, right). Fluorescence is a good technique to visualize chol-rich and chol-poor regions within the membranes because of DPPE-Rhodamine different partition into each phase.

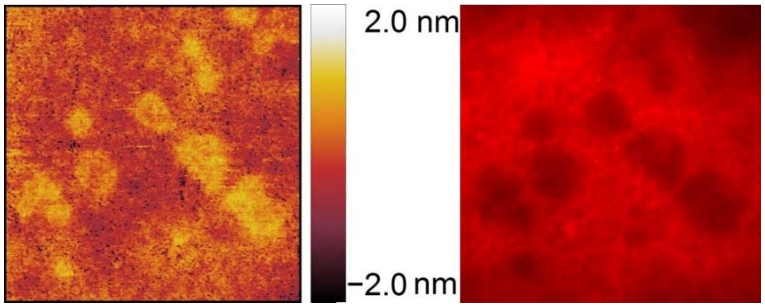

Fig. S6 Correlative AFM-fluorescence images (35 x 35 μm^2) of DPPC:chol 90:10 SLBs on glass, in 20 mM HEPES, 150 mM NaCl, 20 mM $MgCl_2$ buffer solution pH 7.4, at room temperature.

In analogy with Fig. S6, the DPPC:chol 90:10 molar ratio image exposed in Fig. S5 shows the coexistence of chol-rich and chol-poor domains. This result corroborates that the phase behavior of DPPC:chol SLBs on mica[1, 7] and vesicles in suspension[8, 9] and described

in the many phase diagrams reported for the DPPC:chol system[10-13] also occurs on Si-SLBs. It validates the GIXD data presented in Fig. 4 in the main manuscript.

References

1 L. Redondo-Morata, M. I. Giannotti and F. Sanz, *Langmuir*, 2012, **28**, 12851-12860.
2 B. Gumi-Audenis, L. Costa, F. Carla, F. Comin, F. Sanz and M. I. Giannotti, *Membranes*, 2016, **6**.
3 P. E. Milhiet, V. Vié, M.-C. Giocondi and C. Le Grimellec, *Single Molec.*, 2001, **2**, 109-112.
4 B. Gumi-Audenis, F. Sanz and M. I. Giannotti, Soft Matter, 2015, 11, 5447-5454.
5 L. Redondo-Morata, M. I. Giannotti and F. Sanz, *Mol. Membr. Biol.*, 2014, **31**, 17-28.
6 S. Roobol, W. Onderwaater, J. Drnec, R. Felici and J. Frenken, J. App. Crystallogr., 2015, **48**, 1324-1329.
7 P. E. Milhiet, M. C. Giocondi and C. Le Grimellec, *J. Biol. Chem.*, 2002, **277**, 875-878.
8 N. Kucerka, J. D. Perlmutter, J. Pan, S. Tristram-Nagle, J. Katsaras and J. N. Sachs, *Biophys. J.*, 2008, **95**, 2792-2805.
9 J. J. Pan, S. Tristram-Nagle and J. F. Nagle, *Phys. Rev. E*, 2009, **80**.
10 T. P. W. McMullen and R. N. McElhaney, *BBA-Biomembranes*, 1995, **1234**, 90-98.
11 S. Karmakar, V. A. Raghunathan and S. Mayor, *J. Phys.-Condens. Matt.*, 2005, **17**, S1177-S1182.
12 Y.-W. Chiang, A. J. Costa and J. H. Freed, *J. Phys. Chem. B*, 2007, **111**, 11260-11270.
13 D. Marsh, *BBA-Biomembranes*, 2010, **1798**, 688-699.